



Research Article

Received: March 27, 2022

Accepted: April 25, 2022

Published: April 28, 2022

ISSN 2304-6295

Interaction of a unique massive shell with a heterogeneous ground environment during immersion

Perminov, Nikolai Alekseevich¹ 

¹ Emperor Alexander I St. Petersburg State Transport University, St. Petersburg, Russian Federation; perminov-n@mail.ru;

Correspondence:* email perminov-n@mail.ru; contact phone [+79219402684](tel:+79219402684)

Keywords:

Gravitational large-size; Heterogeneous medium unsteady interaction; Differently resistant soils; Stress-strain state regulation; Limit state; Controlled dive

Abstract:

The object of research. The research of interaction regularities of large-size reinforced concrete shells at the erection stages in heterogeneous soil mediums allowed to significantly expand the field of their rational use in underground construction for transport and engineering infrastructure facilities. For a defect-free erection of an underground structure of this type, it is necessary to solve the complex nonlinear design and geotechnical problems together. **Method.** Instability of interaction between a solid structure and ground environment, as well as the heterogeneity of the medium itself, generates a need to create an adaptive control stress-strain state of the system "gravitational large-size body - heterogeneous medium". The geotechnical and structural calculations are used to simulate the interaction of the shell with the ground environment and to predict the adaptive stress-strain control system parameters. The adaptive stress-strain control methods provide conditions for a defect-free lifecycle of the structure during its erection and operation in complex soil and man-made conditions. **Results.** In contrast to the traditional approach, the paper proposes the foundations of a new concept for evaluating the interaction of large size sinking structures in differently resistant soils, taking into account the non-stationarity of the immersion mode.

1 Introduction

During the sinking of large-size tempering structures, specific conditions of their interaction with the ground massif manifest themselves. Due to the inclusion of the scale effect (factor) (by the hyper size of the side surface area of the shell interacting with heterogeneous soil $S=14500\text{m}^2$ and its super large mass $G=1,2 \cdot 10^6\text{kH}$) creating a powerful kinetic momentum at instantaneous, most often sudden, landings of the lowering structure [1], [2]. The joint manifestation of these factors is responsible for the specific, non-linear behavior of the structure during sinking and the host soil mass. The strength and deformability of a large-scale massive structure, its geometric variability should be calculated not only for the final stage of construction. Still for the entire history of immersion, taking into account the history of the interaction of the shell with the soil massif during immersion and consequently the effect of stage-by-stage inheritance of the stress. That can only be done using nonlinear problem solving and computer modeling.

The analysis of the experimental results presented in the article showed that the main defects leading to failure of shell integrity and cracking occurred during the erection of the underground part in the soil mass. Thus, the main task is to ensure the operation of the structure in up to the limit modes at the stage of its life cycle during the erection. In order to be able to realise these conditions, it is crucial to assess the actual structural performance taking into account the process of its stage-by-stage erection in the soil mass under the non-linear material properties of the structure and the ground. These conditions can be taken into account to build a correct model of the interaction history of the shell during its step-

Perminov, N.A.;

Interaction of a unique massive shell with a heterogeneous ground environment during immersion; 2022; *Construction of Unique Buildings and Structures*; **100** Article No 10002. doi: 10.4123/CUBS.100.2

by-step insertion into the soil mass. Calculated justification of the range of preliminary changes in the stress-strain state of the mega massive shell when it is immersed in heterogeneous soils will ensure a defect-free life cycle of the underground structure at the stage of erection [3]. The analysis of the shell loading history at the stage of its erection taking into account the effect of VAT inheritance allows to create an adequate calculation and analytical model of the underground structure and to choose a rational calculation method for predicting the dynamics and spatial boundaries of stress-strain state (SSS) changes in the reinforced concrete shell structure, ensuring defect-free structure at all stages of its immersion.

The purpose of the article is to present a methodological approach for calculating the penetration of large-sized underground drainage structures erected by quenching, to the concept of modeling and forecasting a defect-free life cycle at the stage of their construction. The results of experimental and theoretical studies presented in the article convincingly show that modeling and computational justification of the parameters of preventive protection by geotechnical methods of underground construction at the construction stage will ensure its safety and resistance to man-made impacts at subsequent stages of the life cycle during long-term operation.

2 Materials and methods

According to the results of field and calculated-experimental works and data of complex system of geotechnical monitoring (Fig. 1) of large-sized ($D=50\div 60\text{m}$ and $H=55\div 71\text{m}$) sinking wells the peculiarities of their interaction with heterogeneous soil medium during sinking were studied. The heterogeneity of soil strata is characterized as follows: the upper stratum is represented by quaternary strata to a depth of 14.0-25.0 m (dusty sands of medium density, water-saturated, $E = 11\text{ MPa}$, $C = 0.005\text{ MPa}$, $\varphi = 30^\circ$; dusty loamy sandy loam, $E = 4\text{ MPa}$, $C = 0.01\text{ MPa}$, $\varphi = 15^\circ$; dusty loamy layered fluid plastic, $E = 9\text{ MPa}$, $C = 0.025\text{ MPa}$, $\varphi = 16^\circ$; dusty loamy semi-solid with gravel, pebbles, $E = 14\text{ MPa}$, $C = 0.028\text{ MPa}$, $\varphi = 28^\circ$), the lower one - the roof of Proterozoic clays of dislocated solids ($E = 19\text{ MPa}$, $C = 0.04\div 0.06\text{ MPa}$, $\varphi = 18\div 21^\circ$).

The geomonitoring structure included: 1) program complex of calculations and the geomassive stress under different erection modes; 2) technical means of instrumental observations and SSS control of the separate elements of the system "structure - geomassive"; 3) information-measuring system of gathering, processing, storage and identification of parameters (data) of observations and control; 4) geotechnical methods of the influence on the geometric massif and soil and structure stress.

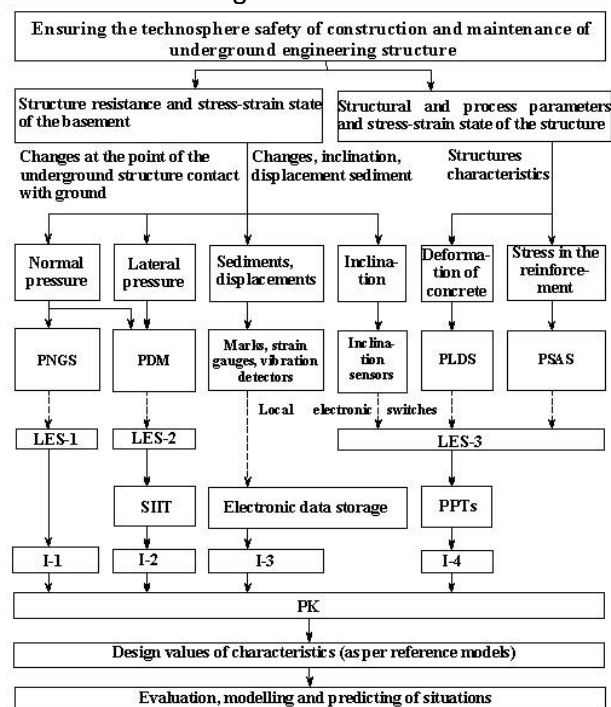


Fig. 1- Hemonitoring and control system for large-sized submersibles downspouts [3]

The monitoring established the peak values of horizontal stresses at the moment of "roll", exceeding the calculated values by more than 2.5 times [4]. This can cause the appearance of microcracks in the concrete structure, which will inevitably lead to violations of waterproofing of the structure. The consequences of this circumstance were noted after 15-20 years of culverts' operation by the inevitable failure of their airtightness.

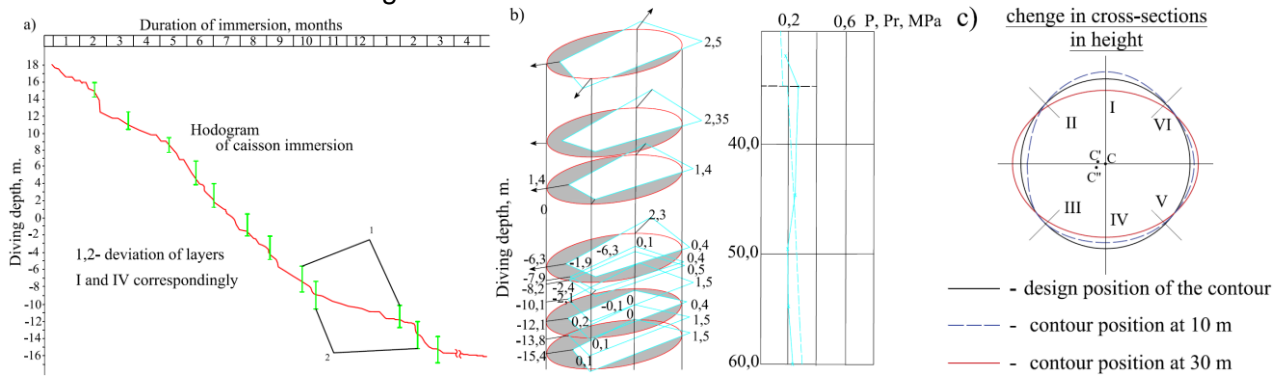


Fig. 2 - Sinking stages and monitoring of the stress-strain state of the large-sized sinking well: a - sinking hodogram; b, c - volume diagram of the shell displacement and the stress-strain state (SSS) of the shell [author's development]

According to the analysis of sinking process and stress-strain state of large-sized shell, different, even alternating, stress-strain state of "large-sized shell-soil mass" system and different types of pressures (Set of rules SP 22.13330.2016. Soil bases of buildings and structures) of ground medium on the shell, including resting pressure, active and passive pressure (see Fig. 3) are observed at different sinking stages.

The strength and deformability of a large-scale massive structure, its geometric variability, must be calculated not only for the final stage of construction, but for the entire history of immersion, taking into account the history of the interaction of the shell with the ground massif during immersion.

According to the general theory [5, 6], the ground pressure on the walls of the well at rest can be determined from the expression:

$$\sigma_o(z) = \sigma_x(z, u_x) \Big|_{u_x=0} = \lambda_0 \gamma z \tag{1}$$

where λ_0 is a coefficient of lateral pressure of the ground at rest; γ is specific weight of the ground; z is distance from the ground surface to the point in question.

At displacements of the manhole shell wall $> 0.005h$ (Set of rules SP 22.13330.2016. Soil bases of buildings and structures p.9.21) from the ground at depth z , the active pressure on the enclosure, σ_a which corresponds to the minimum pressure value, is realized. The passive pressure σ_p , is realized at much larger displacements of the wall on the ground ($U_p = 0,01 - 0,02h$) and corresponds to the maximum value of pressure.

If there is no load on the ground surface, the expressions for determining the active and passive pressures are as follows:

$$\sigma_a(z) = \lambda_a \gamma z - c \lambda_{ac} \tag{2}$$

$$\sigma_p(z) = \lambda_p \gamma z + c \lambda_{pc} \tag{3}$$

where: λ_a - coefficient of active ground pressure;- λ_{ac} coefficient for the influence of ground cohesion on the active pressure; λ_p - coefficient of passive ground pressure;- λ_{pc} coefficient for the influence of ground cohesion on passive pressure; c - specific ground cohesion.

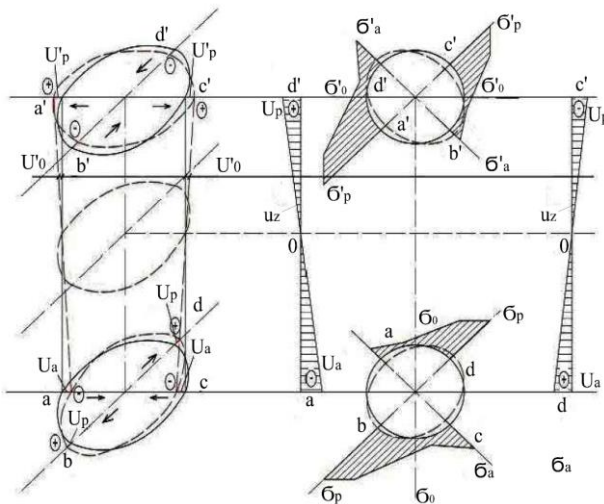


Fig. 3 - Asymmetric deformation (displacement) of the KGOK shell [author's development]

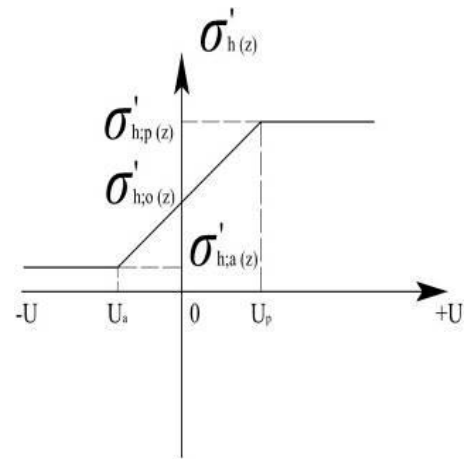


Fig. 4 - Dependence of lateral soil pressure on the shell on displacements $u_x \in (u_p, u_a)$ according to clause 9.21 [Set of rules SP 22.13330.2016. Soil bases of buildings and structures]

The dependence of the effective horizontal pressure of the ground on the retaining structure in the interval $u_x (u_p, u_a)$ has a complex character (Fig. 4) [7].

The active and passive pressures of the ground on the enclosure constitute the pressure limits, that is, the effective pressure is always in the range:

$$\sigma_a(z) \leq \sigma_x(z, u_x) \leq \sigma_p(z) \tag{4}$$

The dependence of the effective horizontal ground pressure on the holding structure in the interval $u_x \in (u_p, u_a)$ has a complex character (Fig.4).

In Fig. 3 and considering Fig. 4 we show the character of asymmetric deformations (displacements) of the shell contour according to the diagram of dependence of horizontal soil pressure on the walls of the well depending on the character of its displacement (asymmetric contraction-expansion of the shell in its upper and lower parts) and the diagram of lateral soil pressure, when approximating it by piecewise linear function.

The function of change of pressure value σ_x at some depth z from displacements can be represented as follows:

$$\sigma_x(u_x) = \begin{cases} \sigma_p, & u_x \leq u_p \\ f(u_x), & u_p < u_x < u_a \\ \sigma_a, & u_a \leq u_x \end{cases} \tag{5}$$

With some assumptions, the function

$$f(u_x) = \sigma_0 - k u_x \tag{6}$$

where k is the stiffness coefficient of the ground; σ_0 - ground pressure at rest.

The ground stiffness coefficient can be used as the ground stiffness coefficient.

The resulting pressure along the bottom and top sections of the well wall is the sum of the effective pressures on both sides of the enclosure. Let us present in the form of two graphs the effective ground pressure on the wall of the well from the ground (left) and the excavation (right) depending on the horizontal displacement of the well shell (Fig. 3).

Construct the function as a $\sigma_x(z, u_x)$ piecewise given function for any value of z .

To describe the effective pressures $\sigma_x(z, u_x)$ for individual sections of the diagram between the active and passive pressure limits $\sigma_a(z) = \lambda_a \gamma z - c \lambda_{ac}$, $\sigma_p(z) = \lambda_p \gamma z + c \lambda_{pc}$, instead of (a), (b), (c), (d) we will use (1), (2), (3), (4), adding indices "l", "r" for the terms relating to the axis of contraction and expansion of the well diameter. In the case where the knife part of the wall of the well is surrounded on both sides by the soil mass $\sigma_x(z, u_x)$ will take the form of:



$$\sigma_x(z, u_x) = \begin{cases} \sigma_p^l(z) - \sigma_a^r(z - h_k), & u_x \leq u_1 \\ \sigma_0^l(z) - \sigma_a^r(z - h_k) - u_x k^l, & u_1 < u_x < u_2 \\ \sigma_0^l(z) - \sigma_a^r(z - h_k) - u_x(k^l + k^r), & u_2 \leq u_x \leq u_3 \\ \sigma_a^l(z) - \sigma_0^r(z - h_k) - u_x k^r, & u_3 < u_x < u_4 \\ \sigma_a^l(z) - \sigma_p^r(z - h_k), & u_4 \leq u_x \end{cases} \quad (7)$$

If we separately consider the resultant pressures on the shell up to the face ($z \leq h_k$), expression (7) will take the form:

$$\sigma_x(z, u_x) = \begin{cases} \sigma_p^l(z), & u_x \leq u_1 \\ \sigma_0^l(z) - k^l u_x, & u_1 < u_x < u_3 \\ \sigma_a^l(z), & u_3 \leq u_x \end{cases} \quad (8)$$

Let us substitute expressions (1), (2), (3) in (7) and (8):

$$\sigma_x(z, u_x) = \begin{cases} \lambda_{pl} \gamma z + c \lambda_{pcl}, & u_x \leq u_1 \\ \lambda_{0l} \gamma z - k_l u_x, & u_1 < u_x < u_3 \\ \lambda_{al} \gamma z + c \lambda_{acl}, & u_3 \leq u_x \end{cases} \quad (9)$$

$$\sigma_x(z, u_x) = \begin{cases} \lambda_p^l \gamma z - \lambda_a^r \gamma (z - h_k) + c \lambda_{pc}^l + c \lambda_{ac}^r, & u_x \leq u_1 \\ \lambda_0^l \gamma z - \lambda_a^r \gamma (z - h_k) + c \lambda_{ac}^r - u_x k^l, & u_1 < u_x < u_2 \\ \lambda_0^l \gamma z - \lambda_a^r \gamma (z - h_k) - u_x(k^l + k^r), & u_2 \leq u_x \leq u_3 \\ \lambda_a^l \gamma z - \lambda_0^r \gamma (z - h_k) - c \lambda_{ac}^l - u_x k^r, & u_3 < u_x < u_4 \\ \lambda_a^l \gamma z - \lambda_p^r \gamma (z - h_k) - c \lambda_{ac}^l - c \lambda_{pc}^r, & u_4 \leq u_x \end{cases} \quad (10)$$

The analysis of formulas (9) and (10) describing resultant pressures shows that practically independent of properties of the host soil mass, the sum of effective pressures on the asymmetric deformed shell (Fig. 3) both in the opposite axial directions and in the lower and upper parts of the shell exhibit a high degree of nonuniformity. As comparative calculations show, the non-uniformity of the resulting pressures can be of the order of one unit (see Figure 5) or more, either on both sides of it, or along the formations of the lower and upper sections of the manhole walls. It is impossible to predict such character of the stress-strain state (SSS) of the "sinking structure-soil massif" system using the recommended calculation approach, as it was noted [8, 9], and it is also impossible to ensure verticality and uniformity of sinking by applying previously known methods of geotechnology [10], as evidenced by hodograms (see Fig. 2a).

The analysis of the conditions of interaction between a massive large-sized shell and the ground massif when immersed in heterogeneous strata testifies to the manifestation of non-stationarity effects in the parameters reflecting this process. In order to be able to study the regularities of manifestation and conditions for preventing their prohibitive development in our further studies, it is necessary to use simulation of shell immersion modes, solving for this purpose the problems in linear and nonlinear formulations.

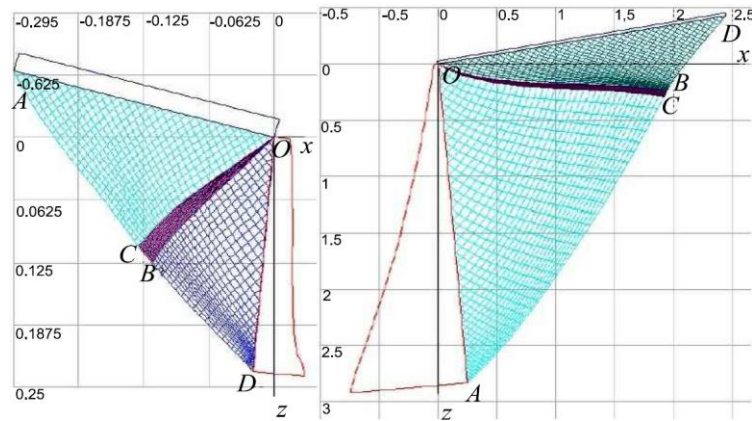


Fig. 5 - Slip lines for active and passive pressures on the retaining wall (by Korolev K.V.) 10Ea<<En [4]

The strength and deformability of a large-scale massive structure, its geometric variability should be calculated not only for the final stage of construction. Still for the entire history of immersion, taking into account the history of the interaction of the shell with the soil massif during immersion and consequently the effect of stage-by-stage inheritance of the stress. That can only be accomplished using nonlinear problem solving, nonlinear models, and computer-based nonlinear modeling.

3 Results and Discussion

3.1 Numerical simulation of the process of correcting the roll of a massive buried structure

In engineering practice, it is known that during the construction of large-diameter manholes there are often problems associated with the deviation of the structure from the design position. The causes of uneven sinking of the well, as it was found in section 2, are peculiarities of interaction of the large-sized shell with heterogeneous soil medium at the stage of its sinking and non-stationary nature of the stress-strain state of the system "large-sized lowering shell - the host soil mass".

By means of numerical geotechnical calculations it is proposed to choose technically possible geotechnological methods for controlling the sinking process: change of the geomassivation in the base of the structure and on the side surface, for example, by methods of prestressing the soil mass, by means of loading leader screens, regulation of the soil resistance on the side surface and other protective geotechnological measures,

In order to assess the effectiveness of geotechnical measures to correct the roll, several series of calculations were carried out on the ground massif with a buried structure. In the initial series of calculations, the soil base was modeled as a linearly deformable medium. In the subsequent series, the nonlinearly deformable material. As a linear medium, a model with a Hooke coupling between stresses and strains was used [11]. An incremental model based on generalized Hooke's law was used to simulate nonlinear material. The relationship between the stress and strain increments is taken separately for the deviatoric and spherical components of the stress tensor.

3.2 Description of the nonlinear ground mode

An incremental strain-type model was used as the computational ground model to solve the nonlinear problem. The relationship between stresses and strains in the model is taken separately for the volumetric and shear components of the stress tensor

$$\left. \begin{aligned} dS_{ij} &= 2G^\delta \cdot de_{ij} \\ d\delta_{cp} &= 3K^\delta \cdot d\varepsilon_{cp} \end{aligned} \right\} \quad (11)$$

Where: dS_{ij} - increment of the deviatoric component of the stress tensor; de_{ij} - increment of the deviatoric component of the strain tensor; $d\delta_{cp}$ - increment of the average stress; $d\varepsilon_{cp}$ - increment of the average strain; K^δ - differential volume strain; G^δ - differential shear strain.

Perminov, N.A.;

Interaction of a unique massive shell with a heterogeneous ground environment during immersion;

2022; *Construction of Unique Buildings and Structures*; **100** Article No 10002. doi: 10.4123/CUBS.100.2



The mathematical approximation of deviator loading is taken as a linear polynomial of two variables:
 - under the condition of loading by the deviatoric component of the stress tensor

$$G_H^{\hat{\sigma}} = A_0 + A_1 \cdot \delta_{cp} + A_2 \cdot \tau_i \quad (12)$$

- under the condition of unloading by the deviatoric component of the stress tensor

$$G_P^{\hat{\sigma}} = A_0 + A_1 \cdot \delta_{cp} \quad (13)$$

Approximation of the differential volume strain modulus under the condition of loading by the spherical component of the stress tensor is carried out by a second-order power polynomial:

$$K_H^{\hat{\sigma}} = B_0 + B_1 \cdot \delta_{cp} + B_2 \cdot \delta_{cp}^2 \quad (14)$$

at "unloading": $K_p = const$

where: τ_i - tangential stress intensity; δ_{cp} - average stress; $A_0; A_1; A_2; K_p; B_0; B_1; B_2$ - model design parameters.

Parameters of the computational model $A_0; A_1; A_2; K_p; B_0; B_1; B_2$ (12-14) were determined from the data of three-axis tests in the stabilometer. The tested soil is a sandy soil of medium coarseness with density $\rho_d=1.65\text{g/cm}^3$ and humidity $W=10\%$.

The procedure for solving the nonlinear problem was reduced to the well-known method of variable stiffness [12, 13], according to which the stiffness matrix was reshaped at each step of the solution according to the current level of SSS and the orientation of the overload vector.

As measures for leveling the roll of a buried structure can be chosen the method of regulation of ground resistance by electroosmosis [14] or the transfer of horizontal pressure on the ground, based on immersion in an array of soil elastic shell, in which by special technology creates excessive pressure, transmitted through the walls of the shell on the ground [15-21]. The elastic casings are placed to some depth along the wall of the buried structure on the outer side. Then pressure is transferred to the inner cavity of the shell, which is transferred to the wall of the structure on one side and to the ground on the other side.

The calculation scheme is a soil mass measuring 296.0 m (horizontal) by 115, 0 m (vertical). In the central part of the scheme is a rigid buried structure having a length of 50.0 m in plan and is buried at 45.0 m.

The computational scheme is discretized into 246 quadrangular isoparametric elements [17], [22-27]. The total number of nodes was 282. The computational domain is represented by two groups of elements with different deformation characteristics. The elements of the first group (rigid buried structure) are represented by an elastic material with an elastic modulus $E=30000.0\text{MPa}$ and Poisson's coefficient $\nu=0.18$.

The surrounding structure space is represented by a group of linearly deformable elements No. 2 with strain modulus $E=30.0\text{MPa}$ and Poisson's coefficient $\nu=0.33$.

In solving the problem, it is assumed that the structure has an initial roll, as shown in Fig. 6 (left to right). To correct for uneven subsidence on the right side of the structure is applied additional load intensity Q on the section of length $L = 12.5\text{m}$.

The load Q in the solved problems was taken equal to 0.3; 0.6 and 0.9 MPa.

Numerical solution of geotechnical problems allowed to obtain the following results. Moving the contour of the dip well in a continuous elastic medium while adjusting the action of the lateral additional load Q and simultaneously adjusting the soil resistance on the lateral surface provided predicted prevention of rolls when sinking in heterogeneous soils. The displacements of the structure according to the solution of the nonlinear problem are shown in Fig. 6. The greatest prevention of absolute horizontal displacement at a load of $Q=0.9\text{MPa}$ is as follows:

1st series of calculations - 48 cm; 2nd series of calculations - 67 cm; 3rd series of calculations - 80 cm; 4th series of calculations - 16 cm.

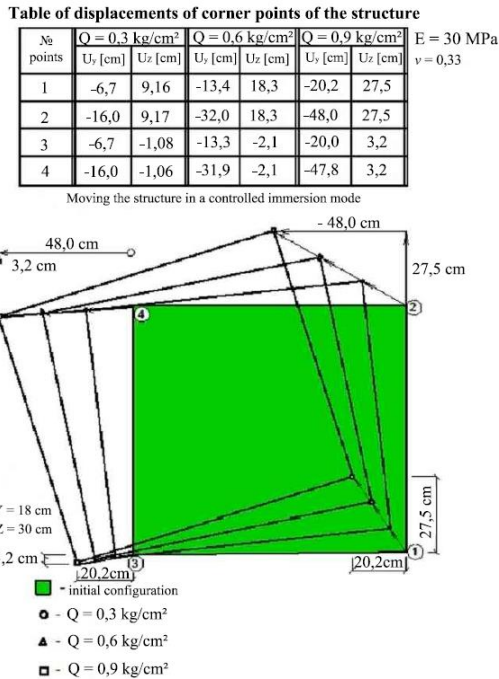


Fig. 6 - Contour displacement of the dip well in a solid elastic medium under the action of lateral load: Q=0.3; 0.6; 0.9 (MPa) [author's development]

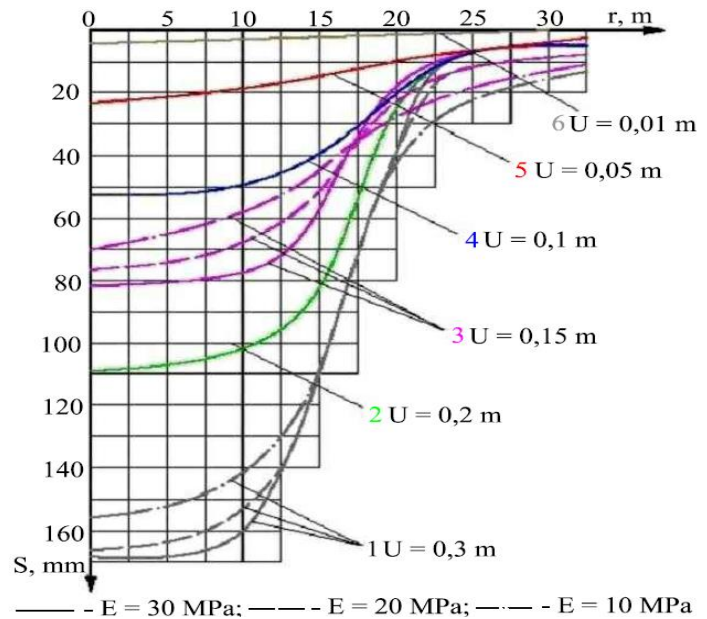


Fig. 7 - Influence of horizontal displacements of manhole walls U_k on ground surface settlements under roll [author's development]

For all solved problems, without the application of geotechnical regulation methods, the irregularity of sinking of the lowered structure was observed: vertical movements (raising (+); lowering (-)) of the left and right contour of the buried structure with the corresponding sign is given below:

Series 1 calculations -3.2 and +27.5 cm; Series 2 calculations -12.5 and +36.4 cm; Series 3 calculations -25.7 and +41.1 cm; Series 4 calculations -3.2 and +15.9 cm.

When the zones with a reduced deformation modulus are taken into account in the calculations (the drilling zone), the horizontal displacement of the upper part of the structure has increased almost 2 times.

By comparing the results for different sizes of the drilling area, it can be seen that for the same E^* , the increase in size by 2 times leads to a displacement increase of about 15-30%.

The geometric dimensions and configuration of the SSS control zones were selected by analyzing the displacement calculation data (Fig.6, 7). When solving the nonlinear problem (4th series of calculations), the displacements were obtained significantly less than when solving elastic problems. This fact can be explained by the considerable deformation heterogeneity in the soil surrounding the buried structure when solving the non-linear problem. The strain modulus when solving a nonlinear problem depends significantly on the stress state. Because of this, the strain modulus increases with depth. We also note that for the nonlinear solution there was no drilling zone, as well as the thixotropic jacket located around the structure was not modeled. The above factors resulted in significantly smaller horizontal displacements when solving the nonlinear problem.

3.3 Modeling of conditionally instantaneous failure of a massive shell when it is immersed in an inhomogeneous soil medium

Using the software package Autodesk Robot Structural Analysis Professional [18], [28-30] we analyzed the performance of the casing structure during its sudden uncontrolled slip (fall) to the bottom of an open soil cavity from a height of 1.3 - 1.5 m at angles of deviation from the vertical axis of 0.5°-5°.

In developing the calculation model (Fig. 9) it was taken into account that the structure of the shell consists of two cylinders stacked on each other: Upper cylinder: outer radius $R = 36$ m, inner radius $R = 30.5$ m, height $H1 = 46$ m; Lower cylinder: outer radius $R = 36$ m, inner radius $R = 30$ m, height $H2 = 25$ m. Thus, the outer diameter of the shell was $D = 72$ m, the height of the shell was $H = 71$ m. Concrete class B30.

To simulate the magnitude of the impact force at failure of the shell in the model, the cylinder fell from a height $H = 150-250$ cm. under the action of its own weight with an angle of inclination of 0.5°-5°

on the compliant soil (clay greenish-gray: $\varphi = 21^\circ$, $C = 0,04$ MPa, $E = 19$ MPa). Spatial shell design scheme was modeled: weight $G = 210000$ t; number of knots 16944; volume finite elements 12496; number of static degrees of freedom: 50828; number of loads 27; free fall acceleration $g = 9.81$ m/kV.s; fall time $t = \sqrt{2 \cdot H/g}$; $\Delta t = 0.30-0.54$ sec. Because of the angle of the slope, the frictional forces were applied at the top of the well on one side and at the bottom on the opposite side.

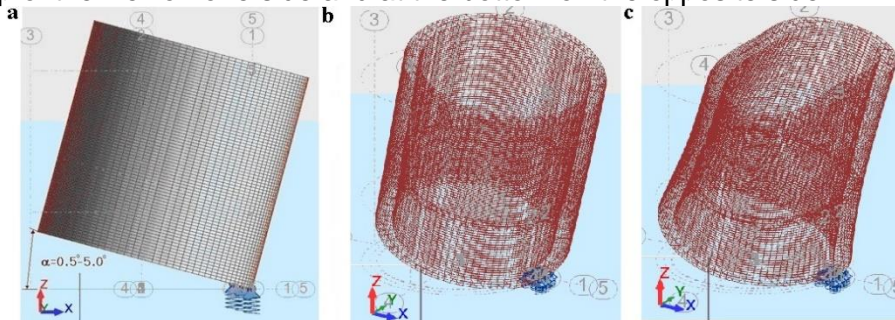


Fig. 8 - Schematics of calculation models and submersible shell simulation results at different angles of its deviation from the vertical axis: a - static support at roll; b,c - failure and slippage at deviation from the vertical axis (roll), respectively: calculation form "N4" at $\alpha=1^\circ$; $\Delta H=1.25$ m ($n=0.56$, $\Delta=26.1$ cm-limited VAT), calculation form "N22" at $\alpha=3.5^\circ$; $\Delta H=2.5$ m ($n=1.94$, $\Delta=183.4$ cm-limited SSS) [author's development]

During the analysis of the shell's deflectivity, we used the coefficient of forbidden state n , defined as the ratio of the equivalent stress of the shell structure according to Mises to the ultimate resistance of concrete of class B30.

Since the simulation of the stalling processes at different deflection angles of the shell from the $-\alpha$ -axis and the drop heights $-\Delta H$ was performed in a rather large range, Figure 8 shows only fragments of the calculated forms "NN4 and 22" and the most characteristic results that were taken for analysis. The total calculation table of the integration results of the motion equations of the shell at stall (fall) at velocity V_Z, V_X, V_Y (cm/sec), acceleration A_Z, A_X, A_Y (cm/sec²) and displacement U_Z, U_X, U_Y (cm) was 186385 lines.

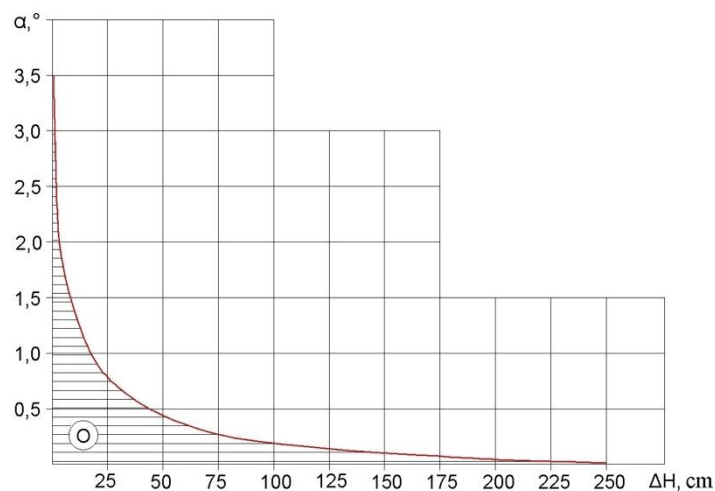


Fig. 9 - Area of maximum permissible values of conditionally instantaneous landings (failures) ΔH of the shell with diameter $D=61$ m, height $H=71$ m, weight $G=210000$ t, at various angles of deviation of the structure from the vertical axis α° (concrete class B30; $\varphi = 21^\circ$, $C = 0,04$ MPa, $E = 19$ MPa) [author's development]

According to the results of modeling (Fig. 9), the acceptable parameters of the spatial position of the shell and the range of its conditionally instantaneous disruptions, providing up to the limit value of the shell's SSS were established [31-33].

The simulation results show that for large-sized shells, the recommendations of normative documents have limited application and need to be confirmed by computational modeling.

4 Conclusion

A new monitoring scheme, geotechnical assessment and numerical simulation of the interaction of a large-sized descending structure with an inhomogeneous soil massif are proposed.

Perminov, N.A.;

Interaction of a unique massive shell with a heterogeneous ground environment during immersion;

2022; *Construction of Unique Buildings and Structures*; **100** Article No 10002. doi: 10.4123/CUBS.100.2



1. The interaction features are characterized by the inclusion of a scale effect (factor): geometric variability (deformations and displacements) of the shell with a hyper-dimensional area of the lateral surface of the exhaust structure interacting with inhomogeneous soil and its super-large mass, creating a powerful kinetic impulse during instantaneous landings of the exhaust structure into inhomogeneous soils that violate its structural safety.

2. The proposed concept makes it possible to simulate the defect-free life cycle of a fallen structure at the design stage by modeling the joint manifestation of factors that determine the specific behavior of the structure when lowering the mass.

3. It is established that at different stages of immersion, a different uniform alternation of the stress-strain state (SSS) of the "large-sized shell-ground mass" system manifests itself and at the same time graphs of the pressure of the soil medium on different parts of the lateral surface of the shell are realized, including resting pressure, active and passive pressure, which cannot be taken into account by traditional calculation methods.

4. The proposed approach, based on the identified features and patterns of interaction of a large-sized lowering structure with an inhomogeneous soil mass, allows us to determine the parameters of geotechnical impacts and modes of their application to prevent the development of shell deformations beyond the limit.

5 Fundings

This work was supported by the RAACS grant No. 2020-CN-7.4.1.

References

1. Il'ichev, V.A., Nikiforova, N.S. Methods for the determination of curvatures and the difference between the slopes of foundations as the criteria of deformation of the basements of buildings and structures. *Soil Mechanics and Foundation Engineering*. 2018. T. 55. No 3. Pp. 168-172. DOI: 10.1007/s11204-018-9521-5.
2. Travush, V.I., Shulyat'ev, O.A. Analysis of the results of geotechnical monitoring of "Lakhta Center" Tower. *Soil Mechanics and Foundation Engineering*. 2019. T. 56. No 2. Pp. 98-106. DOI: 10.1007/s11204-019-09576-9.
3. Perminov, N., Perminov, A. Geotechnical and geocological fundamentals of sustainable life cycle of unique long-operated underground structures of water disposal systems in difficult soil conditions (the experience of St. Petersburg). *Geotechnics fundamentals and applications in construction: new materials, structures, technologies and calculations Proceedings of the International Conference on Geotechnics Fundamentals and Applications in Construction: New Materials, Structures, Technologies and Calculations, GFAC 2019*. Pp. 231-234. DOI: 10.1201/9780429058882-45. Perminov/c4483856e278b688555d5623f6d61b5b3bb71c00 (date of application: 25.04.2022).
4. Karaulov, A.M., Korolev, K.V. On the determination of the maximum earth pressure on retaining walls. *Soil Mechanics and Foundation Engineering*. 2015. T. 52. No 4. Pp. 175-180. DOI: 10.1007/s11204-015-9325-9.
5. Barabash, M., Bashinsky, Y., Korjamins, A. Stress-strain state of the structure in the service area of underground railway. In the collection: *IOP Conference Series: Materials Science and Engineering*. 2017. Pp. 012100. DOI: 10.1088/1757-899X/251/1/012100.
6. Karasev, M.A., Tai Tien, N., Vil'ner, M.A. Forecast of the stress-strain state of the prefabricated lining of underground tunnels of curvilinear cross-section. *Bulletin of the Ural State Mining University*. 2019. № 4 (56). Pp. 90-97. DOI: 10.21440/2307-2091-2019-4-90-97.
7. Perminov, N. Simulation of unsteady interaction of large RC shell with heterogeneous soil milieu for gradually increasing caisson structure. *Geotechnics fundamentals and applications in construction: new materials, structures, technologies and calculations Proceedings of the International Conference on Geotechnics Fundamentals and Applications in Construction: New Materials, Structures, Technologies and Calculations, GFAC 2019*. Pp. 245-249. DOI: 10.1201/9780429058882-48.
8. Lebedev, M.O., Bezrodny, K.P., Larionov, R.I. Ensuring safety during construction of double-track subway tunnels in quaternary deposits. In the collection: *Tunnels and Underground Cities: Engineering and Innovation meet Archaeology, Architecture and Art- Proceedings of the WTC 2019 ITA-AITES World Tunnel Congress*. 45th. 2019. Pp. 941-951. DOI:

Perminov, N.A.;

Interaction of a unique massive shell with a heterogeneous ground environment during immersion;

2022; *Construction of Unique Buildings and Structures*; **100** Article No 10002. doi: 10.4123/CUBS.100.2



- 10.1201/9780429424441-101.
9. Perminov, N. Simulation of defectless lifecycle of unique underground structures of the sewage system at the stage of their construction in difficult soil conditions. *International Journal for Computational Civil and Structural Engineering Publishing House ASV, LTD (Moscow)*. 2019. T. 15. № 1. Pp. 119-130. DOI: 10.22337/2587-9618-2019-15-1-119-130.
 10. Mangushev, R.A., Osokin, A.I. The experience of the underground construction for the complex of buildings on a soft soil in the center of St. Petersburg. *International Journal for Computational Civil and Structural Engineering*. 2020. T. 16. № 3. P. 47-53. DOI: 10.22337/2587-9618-2020-16-3-47-53.
 11. Protosenya, A.G., Karasev, M.A., Belyakov, N.A. Elastoplastic problem for noncircular openings under coulomb's criterion. *Journal of Mining Science*. 2016. T. 52. No 1. Pp. 53-61. DOI: 10.1134/S1062739116010125. Karasev/6719cb945aa9c0f80f85776131d2f970a5844396 (date of application: 25.04.2022).
 12. Ponomaryov, A.B., Kaloshina, S.V., Zakharov, A.V., Bezgodov, M.A., Shenkman, R.I. and Zolotozubov, D.G. Results of geotechnical modeling of the influence of construction of the large foundation ditch on the existing historical building Japanese. *Geotechnical Society Special Publication: the 15th Asian Regional Conf. on Soil Mechanics and Geotechnical Engineering: Geotechnical Heritage. Part 2 (TC 301/ATC 19 Session) 2015. Vol. No 78. Pp. 2676-2679. DOI:10.15593/2224-9826/2014.4.18. Kaloshina/9428e864a7c500eaad2653add766f206fcb2abaa (date of application: 25.04.2022).*
 13. Frolov, Y.S., Konkov, A.N., Larionov, A.A. Scientific Substantiation of Constructive-technological Parameters of St. Petersburg Subway. *Underground Structures Procedia Engineering*, 189. 2017. Pp. 673-680. DOI: 10.1016/j.proeng.2017.05.107.
 14. Ulitsky, V., Bogov, S. Restoration engineering of historic structures: Case study of building 12 on new Holland Island in Saint-Petersburg. *Geotechnics Fundamentals and Applications in Construction: New Materials, Structures, Technologies and Calculations - Proceedings of the International Conference on Geotechnics Fundamentals and Applications in Construction: New Materials, Structures, Technologies and Calculations, GFAC 2019. Pp. 390-395. DOI: 10.1201/9780429058882-75.*
 15. Protosenya, A.G., Karasev, M.A., Belyakov, N.A., Lebedev, M.O. Geomechanics of low-subsidence construction during the development of underground space in large cities and megalopolises. *International Journal of Mechanical and Production Engineering Research and Development*. 2019. T. 9. No 5. Pp. 1005-1014. DOI: 10.24247/ijmperdoct201989.
 16. Ledyayev, A., Kavkazskiy, V., Vatulin, Y., Svitin, V., Shelgunov, O. Mathematical modeling of aerodynamic processes in railway tunnels on high-speed railways. *E3S Web of Conferences*, 157, 6017 (2020). DOI: 10.1051/e3sconf/202015706017.
 17. Merzlyakov, V.P., Vlasov, A.N. Effect of polygonal crack nets on the deformation characteristics of rocks. *Soil mechanics and foundation engineering*. 1993. No 30(3). Pp. 85-91. DOI: 10.1007/BF01712792.
 18. Perelmuter, A.V., Fialko, S.Y. Inelastic analysis of reinforced concrete structures in SCAD. *International Journal for Computational Civil and Structural Engineering Publishing House ASV, LTD (Moscow)*. 2019. T. 15. No 1. Pp. 54-60. DOI: 10.22337/2587-9618-2019-15-1-54-60.
 19. Nikiforova, N.S., Konnov, A.V., Nguyen, Van Hoa, Prostotina, L.A. The influence of the device of cut-off screens made using jet technology on the sediment of the surrounding buildings. *Housing construction*. 2019. No 7. Pp. 3-8. DOI: 10.31659/0044-4472-2019-7-3-8.
 20. Nguyen, Van Hoa, Nikiforova, N.S. The choice of soil models in design of deep excavation in soft soils of Viet Nam. *MATEC Web of Conferences*. 2018. Vol. 251. No 04033. DOI: 10.1051/matecconf/201825104033.
 21. Nikiforova, N.S., Nguyen, Van Hoa. Calculating the maximum pressure on the diaphragm wall subjected to seismic loading accounting for geotechnical conditions of Vietnam. *IOP Conference Series: Materials Science and Engineering*. 2020. No 869. 072032. DOI: 10.1088/1757-899X/869/7/072032.
 22. Bulychev, N.S., Fotieva, N.N. Theory and practice of tunnel lining design. *Modern tunneling science and technology*. 2017. Pp. 445-450. DOI: 10.1201/9780203746653-76.
 23. Bogomolov, A.N., Bogomolova, O.A., Ushakov, A.N. Analysis of the stress state at the contours of underground horizontal mine workings exposed to uniform pressure and determination of the safe laying depth. *Soil Mechanics and Foundation Engineering*. 2022. T. 58. No 6. Pp. 507-510.

Perminov, N.A.;

Interaction of a unique massive shell with a heterogeneous ground environment during immersion;

2022; *Construction of Unique Buildings and Structures*; **100** Article No 10002. doi: 10.4123/CUBS.100.2



- DOI: 10.1007/s11204-022-09773-z.
24. Yevtushenko, S.I., Kalafatov, D.A. The work of the foundation with the shell in conditions of a constrained lateral strut. *Construction and architecture*. 2022. Vol. 10. No 1. Pp. 21-25. DOI: 10.29039/2308-0191-2021-10-1-21-25.
 25. Wells, T., Melchers, R.E. Modelling concrete deterioration in sewers using theory and field observations. *Cement and Concrete Research*. 77. 2015. Pp. 82-96. DOI:10.1016/J.CEMCONRES.2015.07.003.
 26. Korovkin, V.S. Engineering kinematic theory in application to the calculation of pile foundations. *Magazine of Civil Engineering*. 2017. No 2(70). Pp. 57-71. DIO: 10.18720/MCE.70.6.
 27. Shmidt, O.A. Improvement of a method for calculating the settlement of pile foundations of tanks during their exploitation. *Bulletin of PNRPU. Construction and Architecture*. 2018. Vol. 9. No 2. Pp. 125-133. DOI: 10.15593/2224-9826/2018.2.12.
 28. Ter-Martirosyan, Z.G., Bakhmisov, V.V. To the question of concrete creep in the soil environment. *Vestnik MGSU [Monthly Journal on Construction and Architecture]*. 2020. Vol. 15(9) Pp.1285-1296. DOI: 10.22227/1997-0935.2020.9.1285-1296.
 29. Kim, D., Kim, H., Shin, K.J., Seo, H. The effect of concrete deformation on displacement of an axially loaded drilled shaft. *Marine Georesources & Geotechnology*. 2016. Vol. 34. Issue 2. Pp. 116–126. DOI: 10.1080/1064119x.2014.969413.
 30. Khodzhaev, D., Vatin, N., Abdikarimov, R., Normuminov, B., Mirzaev, B. Dynamic stability of viscoelastic orthotropic shells with concentrated mass. In the collection: *IOP CONFERENCE SERIES. Materials Science and Engineering*. Kazan, Russia, 2020. Pp. 012042. DOI: 10.1088/1757-899X/890/1/012042.
 31. Travush, V.I., Karpenko, N.I., Erofeev, V.T., Vatin, N., Erofeeva, I.V., Maksimova, I.N., Kondrashchenko, V.I., Kesarijskij, A.G. Destruction of powder-activated concrete with fixation of destruction by a laser interferometer. *Magazine of Civil Engineering*. 2020. No 3(95). Pp. 42-48. DOI: 10.18720/MCE.95.4.
 32. Nuguzhinov, Zh., Vatin, N., Bakirov, Zh., Khabidolda, O., Zholmagambetov, S., Kurokhtina, I. Stress-strain state of bending reinforced beams with cracks. *Magazine of Civil Engineering*. 2020. No 5 (97). Pp. 9701. DOI: 10.18720/MCE.97.1.
 33. Kanyukova, S., Vatin, N., Leybman, D., Sazonova, T. Dynamic control method of design terms in underground construction. In the collection: *Procedia Engineering*. 2016. Pp. 1918-1924. DOI: 10.1016/j.proeng.2016.11.942.